

p125A exists as part of the mammalian Sec13/Sec31 COPII subcomplex to facilitate ER-Golgi transport

Yan Shan Ong,¹ Bor Luen Tang,² Li Shen Loo,¹ and Wanjin Hong^{1,2}

¹Cancer and Developmental Cell Biology Division, Institute of Molecular and Cell Biology, Singapore 138673, Singapore

²Department of Biochemistry, Yong Loo Lin School of Medicine, National University of Singapore, Singapore 119077, Singapore

Coat protein II (COPII)-mediated export from the endoplasmic reticulum (ER) involves sequential recruitment of COPII complex components, including the Sar1 GTPase, the Sec23/Sec24 subcomplex, and the Sec13/Sec31 subcomplex. p125A was originally identified as a Sec23A-interacting protein. Here we demonstrate that p125A also interacts with the C-terminal region of Sec31A. The Sec31A-interacting domain of p125A is between residues 260–600, and is therefore a distinct domain from that required for interaction with

Sec23A. Gel filtration and immunodepletion studies suggest that the majority of cytosolic p125A exists as a ternary complex with the Sec13/Sec31A subcomplex, suggesting that Sec 13, Sec31A, and p125A exist in the cytosol primarily as preassembled Sec13/Sec31A/p125A heterohexamers. Golgi morphology and protein export from the ER were affected in p125A-silenced cells. Our results suggest that p125A is part of the Sec13/Sec31A subcomplex and facilitates ER export in mammalian cells.

Introduction

To begin their journey along the biosynthetic/secretory pathway, proteins that have entered the ER and are destined for the Golgi apparatus or beyond must first exit the ER (Gorelick and Shugrue, 2001; Ellgaard and Helenius, 2003; Mancias and Goldberg, 2005; Hughes and Stephens, 2008). ER export is mediated by vesicle formation at specialized ER domains known as the ER exit sites (ERES) by the coat protein II (COPII) complex. The first mechanistic understanding of the function of various components of COPII pertaining to vesicle formation came from studies on the yeast system (Kuehn et al., 1998). We now have a fairly good understanding of the molecular and structural interactions that drive COPII assembly (Tang et al., 2000; Gürkan et al., 2006; Bi et al., 2007; Kirk and Ward, 2007; Fromme and Schekman, 2008; Stagg et al., 2008). COPII subunits must first be recruited to the correct sites on the ER membrane, i.e., that of the ERES. The COPII coat is formed through sequential binding of three cytosolic components, a small GTPase Sar1 (Nakano and Muramatsu, 1989; Barlowe et al., 1993), the Sec23/Sec24 heterodimer complex (Hicke et al., 1992), and the Sec13/Sec31

heterotetramer complex (Salama et al. 1993) to the ERES. The sequence of COPII protein assembly was established by the sequential addition of yeast COPII components to an *in vitro* ER vesicle budding assay. This order of assembly was subsequently confirmed in mammalian cells (Barlowe et al., 1994; Kuge et al., 1994; Aridor et al., 1995; Lee et al., 2004). Even though COPII vesicle formation could be minimally reconstituted using purified yeast COPII proteins (Matsuoka et al., 1998), additional regulatory factors such as Sec16p (Espenshade et al., 1995; Gimeno et al., 1996; Shaywitz et al., 1997; Supek et al., 2002) and Sed4p (Gimeno et al., 1995; Saito-Nakano and Nakano, 2000) were found to contribute to the rate and efficiency of COPII-mediated protein export from the ER.

For each of the yeast COPII genes identified, there exist at least two or more homologous forms in mammals (Barlowe, 2003). The presence of multiple isoforms in higher organisms brings about combinatorial diversity for COPII vesicle formation, indicating a greater range of complexity in the regulation of COPII-mediated protein export. Therefore, a comprehensive

Correspondence to Wanjin Hong: mcbhwj@imcb.a-star.edu.sg

Abbreviations used in this paper: BFA, brefeldin A; COPII, coat protein II; ERES, ER exit site; GT, β 1,4-galactosyl transferase; ManII, mannosidase II; VSV, vesicular stomatitis virus; VSVG, VSV G protein.

© 2010 Ong et al. This article is distributed under the terms of an Attribution-Noncommercial-Share Alike-No Mirror Sites license for the first six months after the publication date (see <http://www.rupress.org/terms>). After six months it is available under a Creative Commons License (Attribution-Noncommercial-Share Alike 3.0 Unported license, as described at <http://creativecommons.org/licenses/by-nc-sa/3.0/>).

understanding of ER export in mammalian cells would depend on detailed biochemical and functional characterization of mammalian COPII proteins and their regulatory proteins.

The Sec13/Sec31 subcomplex is the last of the COPII components to be recruited onto membranes before vesicle formation, and may be linked to components of regulatory mechanisms that govern ER exit. We have previously shown that rat liver cytosol depleted of proteins that could potentially interact with the C-terminal fragment of Sec31A was defective in ER-Golgi transport of vesicular stomatitis virus (VSV) G protein (VSVG) in a semi-intact cell assay (Tang et al., 2000). This observation indicates that a cytosolic factor(s) sequestered by the C-terminal fragment of Sec31A is likely important for ER export of VSVG.

p125A was first described as a Sec23-interacting peripheral protein of 125 kD with phospholipase A₁ homology (Tani et al., 1999) and is enriched in the ERES, but the functional importance is unknown (Shimoi et al., 2005). The mammalian genome contains a p125A parologue, p125B, which lacks the proline-rich N-terminal domain (1–372 residues) that is required for Sec23 interaction. The sequence homology is confined to region of residues 373–628 of p125A having an overall 52% sequence identity with the homologous region of p125B. p125B does not interact with Sec23 and its function is unclear, although it is a new member of the phosphatidic acid–preferring phospholipase A₁ family (Nakajima et al., 2002). p125A was recruited to the ERES in an active Sar1p-dependent manner. Overexpression of p125A causes ERES clustering at the perinuclear region (Tani et al., 1999; Shimoi et al., 2005). Our results here show that p125A is a Sec31A-interacting protein and likely part of a Sec13/Sec31A/p125A heterohexameric complex that facilitates ER-Golgi transport.

Results

p125A as a Sec31A-interacting protein

Our previous study showed that the C-terminal 180-residue region of Sec31A expressed as a GST fusion protein (GST-Sec31A) inhibited in vitro transport of VSVG from the ER to the Golgi (Tang et al., 2000). One possible explanation is that GST-Sec31A sequesters important protein(s) that interact with endogenous Sec31A. To explore this hypothesis, GST-Sec31A was used in pull-down experiments to identify possible Sec31A-interacting proteins. As shown in Fig. 1 A, several polypeptides from the rat liver cytosol were retained by immobilized GST-Sec31A (lane 3) but not by GST (lane 2). Mass spectrometric analysis revealed that one of the bands is p125A (as indicated). Because p125A was originally identified as an interacting protein for Sec23A (Tani et al., 1999), we subsequently focused on its interaction with Sec31A and the functional relevance of such an interaction. Coimmunoprecipitation experiments validated the interaction between Sec31A and p125A (Fig. 1 B). When GFP-Sec31A was coexpressed with myc-p125A, antibodies against myc can efficiently coimmunoprecipitate GFP-Sec31A (lanes 2 and 5). The coimmunoprecipitation is dependent on the coexpression of myc-p125A (lanes 3 and 6).

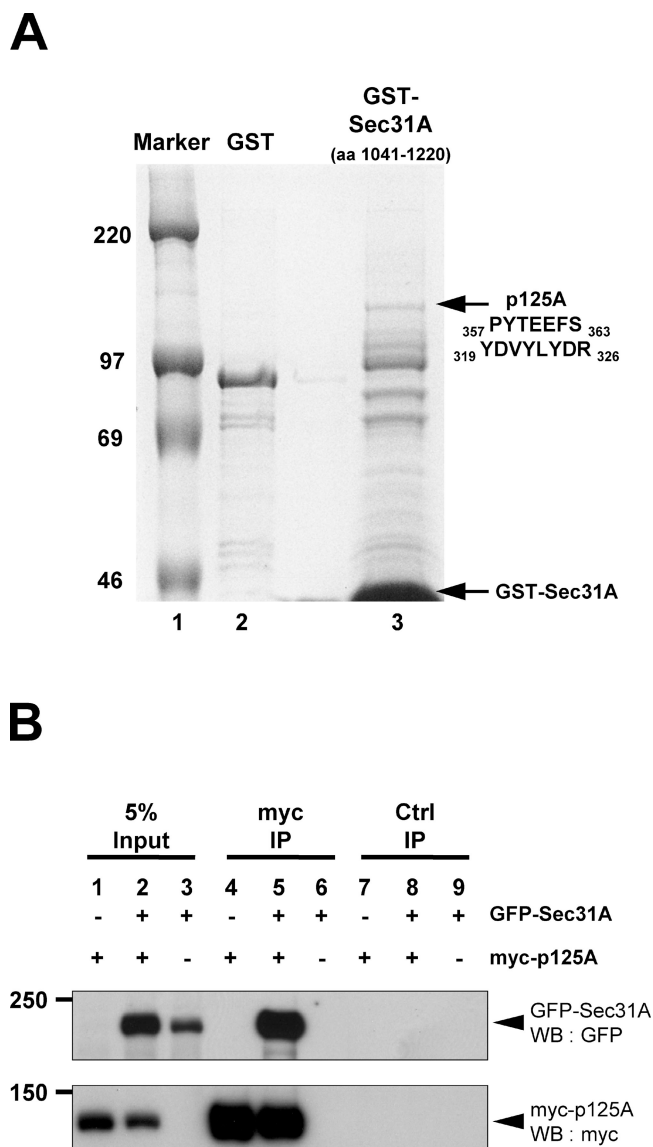


Figure 1. p125A binds to Sec31A. (A) GST-Sec31A and GST immobilized onto glutathione beads were incubated with rat liver cytosol and proteins retained on the beads were eluted and resolved on a 7% SDS-PAGE gel. Distinct bands were cut out and subjected to protein identification by mass spectrometry. Arrow indicates mammalian p125A with the identified peptide sequences shown. (B) myc-p125A and GFP-Sec31A were exogenously expressed in HEK293 cells either singly or in combination as indicated. Cell lysates were prepared and subjected to immunoprecipitation by either anti-myc (9E10) antibodies or control mouse IgG. The samples (together with 5% starting materials as controls) were resolved by SDS-PAGE and transferred to PVDF and immunoblotted using antibodies against GFP and myc. Molecular size markers are in kD.

p125A exists as part of mammalian Sec13/Sec31 subcomplex in the cytosol

Sec13 (33 kD) and Sec31A (140 kD) are believed to exist in the cytosol as heterotetramer and have a predicted combined molecular weight of ~370 kD. However, the Sec13/Sec31 complex has been reported to be fractionated to higher molecular weight regions of ~600–700 kD (Salama et al., 1993, 1997; Shugrue et al., 1999; Tang et al., 2000; Kim et al., 2001; Lederkremer et al., 2001). Biochemical and electron microscopy studies indicate that the heterotetramer complex exists as an elongated rod-like

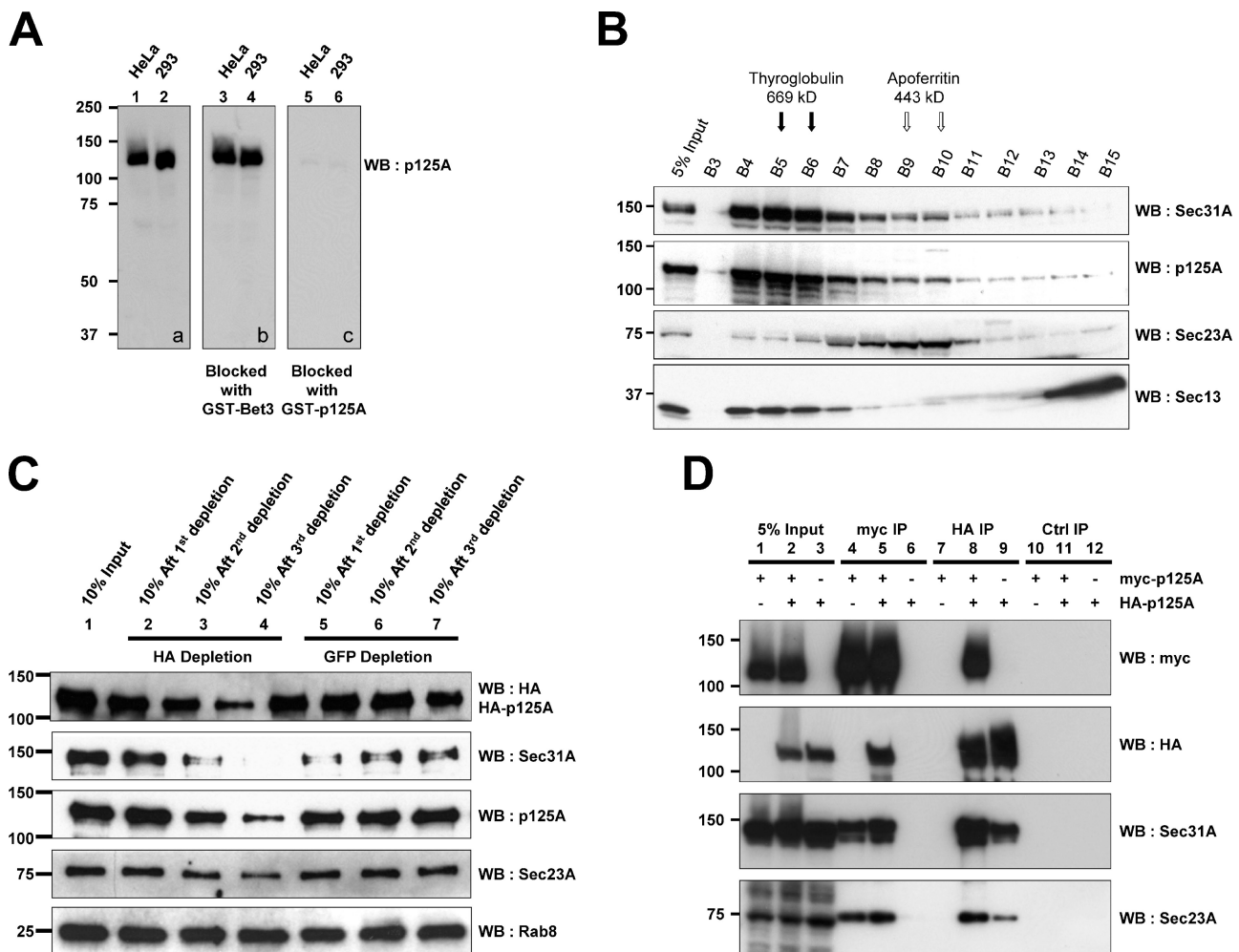


Figure 2. p125A exists as a ternary complex with the Sec13/Sec31A heterotetramer in the cytosol. (A) Characterization of p125A antibodies. Residues 500–758 of p125 were expressed as fusion protein with GST (GST-p125A) and used to raise rabbit antibodies. Affinity-purified antibodies were used for immunoblot analysis. 30 µg of HeLa cell (lanes 1, 3, and 5) and HEK293 cell lysate (lanes 2, 4, and 6) were loaded per lane. The lysates were resolved on SDS-PAGE, transferred to PVDF membrane, and then subjected to immunoblot analysis using anti-p125A antibodies. For the second and third panels, anti-p125A antibodies were preincubated with 500 µg of recombinant GST-Bet3 and GST-p125A, respectively. (B) p125A fractionated with Sec31A and Sec13 in gel filtration. HeLa cell cytosol was subjected to gel filtration in Superose 6 at a flow rate of 0.3 ml/min. Fractions (0.6 ml each) were collected and then TCA precipitated. The proteins were subjected to SDS-PAGE and transferred to PVDF and immunoblotted using antibodies against Sec31A, p125A, Sec23A, and Sec13 as indicated. The arrows indicate the fractions in which the molecular weight markers peaked. (C) Sec13A is co-immunodepleted with p125A. Cytosol was prepared from HEK293 cells transfected to express HA-p125A. The cytosol was subjected to three consecutive cycles of immunodepletion using anti-HA or control anti-GFP antibody-conjugated beads. One tenth of the cytosol was collected and TCA precipitated after each round of immunodepletion. The proteins (along with the cytosol before immunodepletion) were subjected to SDS-PAGE and transferred to PVDF and immunoblotted using antibodies against HA, Sec31A, p125A, Sec23A, and Rab8. Sec31A and total p125A were efficiently and proportionally depleted along with HA-p125A. (D) p125A exists in a multimeric form. myc-p125A and HA-p125A were exogenously expressed in transfected HEK293 cells either singly or in combination as indicated. Cell lysates were subjected to immunoprecipitation with anti-myc (lanes 4–6), anti-HA (lanes 7–9), and control mouse IgG (lanes 10–12). The immunoprecipitates, along with the starting materials, were resolved on SDS-PAGE and analyzed by immunoblot with antibodies against myc, HA, Sec31A, and Sec23A. Molecular size markers are in kD.

structure (Lederkremer et al., 2001; Matsuoka et al., 2001; Stagg et al., 2006; Fath et al., 2007), which may be responsible for them to fractionate at a higher molecular weight in gel filtration (Siegel and Monty, 1966). Additionally, association of other proteins with this heterotetrameric complex may also contribute to this observation. Because p125A was pulled down from rat liver cytosol by GST-Sec31A, p125A may be part of this Sec13/Sec31A complex and should coelute in similar fractions with Sec13 and Sec31A in a gel filtration assay. To facilitate our studies on endogenous p125A, we have raised rabbit antibodies using a recombinant fragment covering residues 500–758 of p125A. These polyclonal antibodies react specifically with

p125A in immunoblot (Fig. 2 A) and by immunolabeling (see Fig. 4 A). As shown in Fig. 2 B, the majority of p125A coeluted with Sec31A and Sec13 in fractions B4 to B7, which corresponds to ~600–700 kD in size as marked by thyroglobulin (669 kD). Similarly, the majority of Sec31A and Sec13 are present in these fractions, with some Sec13 also being detected in low molecular weight fractions (B14–B15). Consistent with published data (Mizoguchi et al., 2000), p125A did not cofractionate with Sec23A. Most of Sec23A was eluted in fractions B7 to B11, which is closer to the size of apoferritin (400 kD). If two molecules of p125A are associated with Sec13/Sec31A heterotetramer, then the estimated size of the complex will be ~600 kD.

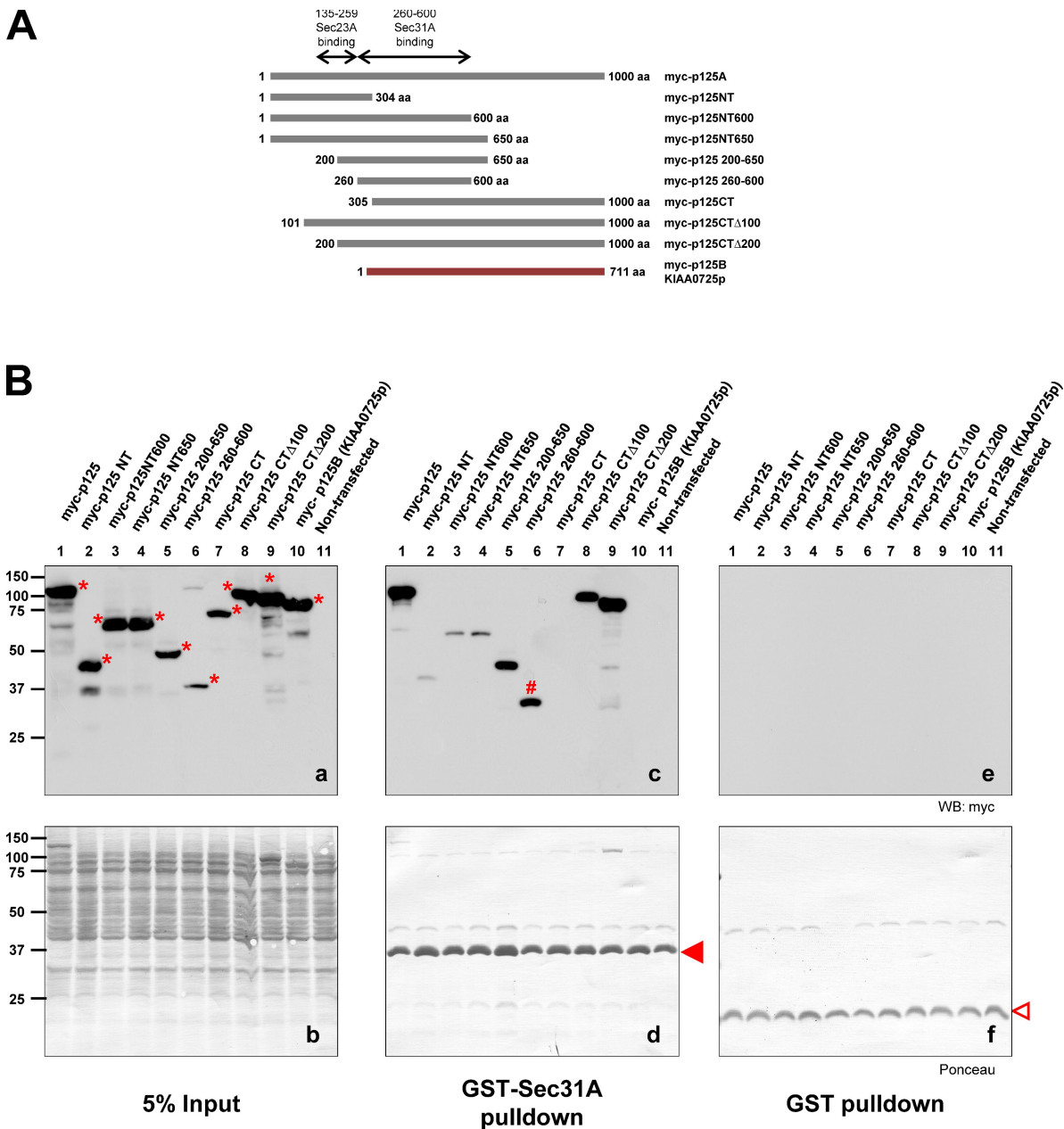


Figure 3. Residues 260–600 of p125A are sufficient for binding to Sec31A. (A) a schematic illustration of p125A deletion constructs. cDNA fragments encoding various mutants were generated by PCR and validated by sequencing. The fragments were digested with Sall and NotI and then subsequently cloned into pDmyc-neo. KIAA0725p, the homologue of p125A, also known as myc-p125B (Nakajima et al., 2002), is also indicated. (B) myc-p125A deletion constructs were transfected into HEK293 cells. Cell lysates were prepared and subjected to pulldown using immobilized GST-Sec31A and GST. Proteins retained by the beads, along with cell lysates, were subjected to SDS-PAGE, transferred to PVDF membrane, and immunoblotted using anti-myc antibody. Red asterisk indicates the expected sizes of the various HA-tagged mutants; red hash indicates the smallest fragment that could be pulled down by GST-Sec31A. Solid red triangle indicates GST-Sec31A, and the empty red triangle represents GST. b, d, and f are Ponceau staining of the immunoblots. Molecular size markers are in kD.

It is thus conceivable that the majority of Sec13/Sec31 exists as a stable heterohexameric complex with p125A in the cytosol.

An immunodepletion experiment was performed using cytosol prepared from cells stably expressing HA-tagged p125A. As shown in Fig. 2 C, HA-p125A could be efficiently depleted after three consecutive immunoprecipitation steps. Interestingly, the levels of endogenous Sec31A and total p125A were also proportionally reduced, suggesting that exogenously expressed HA-p125A and endogenous Sec31A exist in the same protein complex in the cytosol. The reduced level of total p125A implies

that HA-p125A may interact with endogenous p125A because HA-p125A, being only 3 kD larger, was not resolvable from the endogenous p125A by SDS-PAGE. On the other hand, Sec23A, which is known to interact with p125A (Tani et al., 1999), was not immunodepleted as significantly as Sec31A and total p125A, which is consistent with the earlier result that it fractionated differently from p125A in the cytosol. These results imply that Sec23A and p125A probably do not interact in the cytosol, and their interaction may occur preferentially on the membrane. Rab8 (Huber et al., 1993) was used as a negative control.

The ability of anti-HA-p125A antibodies to also deplete total (and thus also endogenous) p125A suggests that more than one molecule of p125A is present in the complex with Sec31A, and that p125A may be able to interact with itself either directly or indirectly via interaction with Sec31A. Using two different epitope-tagged versions of p125A, reciprocal coimmunoprecipitation experiments were performed. As shown in Fig. 2 D, when myc-p125A and HA-p125A were coexpressed (lane 2), antibodies against either myc (lane 5) or HA (lane 8) could recover both forms of tagged p125 in addition to the recovery of Sec31A and Sec23A from total cell lysate. HA-p125A, Sec31A, or Sec23A was not recovered by anti-myc antibodies when myc-p125 was not coexpressed (lane 6). Similarly, myc-p125A, Sec31A, or Sec23A was not recovered by anti-HA antibodies when HA-p125 was not coexpressed (lane 7). These results suggest that some HA-p125A and myc-p125A are present in the same complex with Sec31A. The coimmunoprecipitation of Sec23A with tagged p125A in this experiment suggests that a membrane-bound pool of p125A was precipitated, implying that p125A is likely interacting simultaneously with Sec31 and Sec23 on the membrane in addition to self-interaction. These results suggest that Sec13, Sec31A, and p125A preferentially exist as a stable heterohexamer in the cytosol. Once recruited onto the membrane, they can then engage the Sec23A/Sec24 subcomplex.

Residues 260–600 of p125A are mostly responsible for its interaction with Sec31A

To define the region of p125A that is responsible for its interaction with Sec31A, expression constructs for eight different fragments of p125A (Fig. 3 A) were generated. Together with constructs expressing full-length p125A and p125B, they were subjected to pull-down assays using GST-Sec31A. As shown in Fig. 3 B, all proteins were successfully expressed (left panels). Consistently, myc-p125A (lane 1) but not myc-p125B (lane 10) was recovered by immobilized GST-Sec31A (middle panels). Deletion of its N-terminal 304 residues completely disrupted its interaction with Sec31A (lane 7), although this N-terminal 304-residue region was not itself sufficient for Sec31A interaction (lane 2). Deletion of the N-terminal 100 or 200 residues did not affect the interaction (lanes 8 and 9, respectively). The N-terminal fragments consisting of residues 1–600 or 1–650 were retained by GST-Sec31A (lanes 3 and 4, respectively). Furthermore, the fragment consisting of residues 260–600 was efficiently retained by GST-Sec31A (lane 6). Further deletion using this fragment resulted in disruption of its ability to interact with Sec31A, suggesting that residues 260–600 encompass the determinant for p125A to interact with Sec31A. Because a previous study has defined the region consisting of residues 135–250 as being responsible for p125A's interaction with Sec23A (Mizoguchi et al., 2000), these results suggest that p125A interacts with Sec23A and Sec31A using different regions. As such, p125A may have the potential to interact with Sec23A and Sec31A simultaneously, which is consistent with coimmunoprecipitation results (Fig. 2 D).

p125A is enriched in the ERES

Using rabbit antibodies against p125A for indirect immunofluorescence microscopy, p125A labeling decorated numerous

vesicular structures enriched in the perinuclear region with some being scattered around the cell periphery (Fig. 4 A, a). The labeling was abolished by prior incubation of the antibodies with the recombinant antigen (Fig. 4 A, g), but not by prior incubation with unrelated GST-Bet3 (Fig. 4 A, d). Double labeling using rabbit anti-p125A and mouse anti-Sec31A antibodies revealed that the majority of p125A-labeled vesicular structures are also positive for Sec31A (Fig. 4 B). The colocalization of p125A with Sec31A is very extensive and is consistent with the notion that p125A interacts with Sec31A not just in the cytosol, but also on specific membranes. These results suggest that, like other COPII components, endogenous p125A is enriched in the ERES.

Live imaging of cells coexpressing p125A-Cherry and Sec31A-GFP showed that they are extensively colocalized (Fig. 4 C). p125A-Cherry and Sec31A-GFP are associated with each other quite stably over the observed period of 30 min (Fig. 4 D). The spotty ERES structures marked by Sec31A-GFP and p125A-Cherry were in constant motion and were sometimes observed to participate in homotypic fusion (illustrated by time-lapse sequences in Fig. 4 E for the boxed region in Fig. 4 D). These results suggest that p125A functions in close association with COPII coat components.

p125A depletion by RNAi caused fragmentation and dispersion of the Golgi apparatus

To investigate the cellular role of p125A, RNAi was used to knock down its expression. As shown in Fig. 5 A, p125A was efficiently knocked down by p125A-specific siRNA (lane 1), whereas the levels of Sec31A, Sec23A, and Sec13 were not significantly affected (lane 4). siRNA for Sec13 not only efficiently decreased the level of Sec13, but also significantly reduced the level of Sec31A (lane 3), suggesting that the stability of Sec31A might be dependent on its interaction with Sec13. Silencing Sec31A by its siRNA, however, did not significantly affect the level of Sec13 (lane 2). This is in agreement with the fractionation data in Fig. 2 B, which showed that a substantial amount of Sec13 in the cytosol exists as low molecular weight (presumably monomeric) forms.

The cellular distribution of Sec31A was noticeably affected in p125A-silenced cells, and vice versa (Fig. 5 B). In comparison to control cells treated with nontarget siRNA (panels a–c), upon p125A knockdown (panels d–f), Sec31A labeling in the perinuclear region appeared more diffused (panel e). Furthermore, the background labeling for Sec31A (likely reflecting distribution of Sec31A in the cytosol) seemed increased in p125A knockdown cells. In cells where Sec31A is silenced (panels g–i), p125A seemed to be more concentrated around the perinuclear region with an elevated background (likely cytosolic) labeling. p125A labeling in the peripheral vesicular structures was mostly reduced. These results indicate that the normal distribution of Sec31A and p125A in the ERES may be influenced by the presence of each other.

The role of p125A in maintaining normal Golgi structure was first investigated by examining the effect of its depletion on the distribution of the Golgi β 1,4-galactosyl transferase

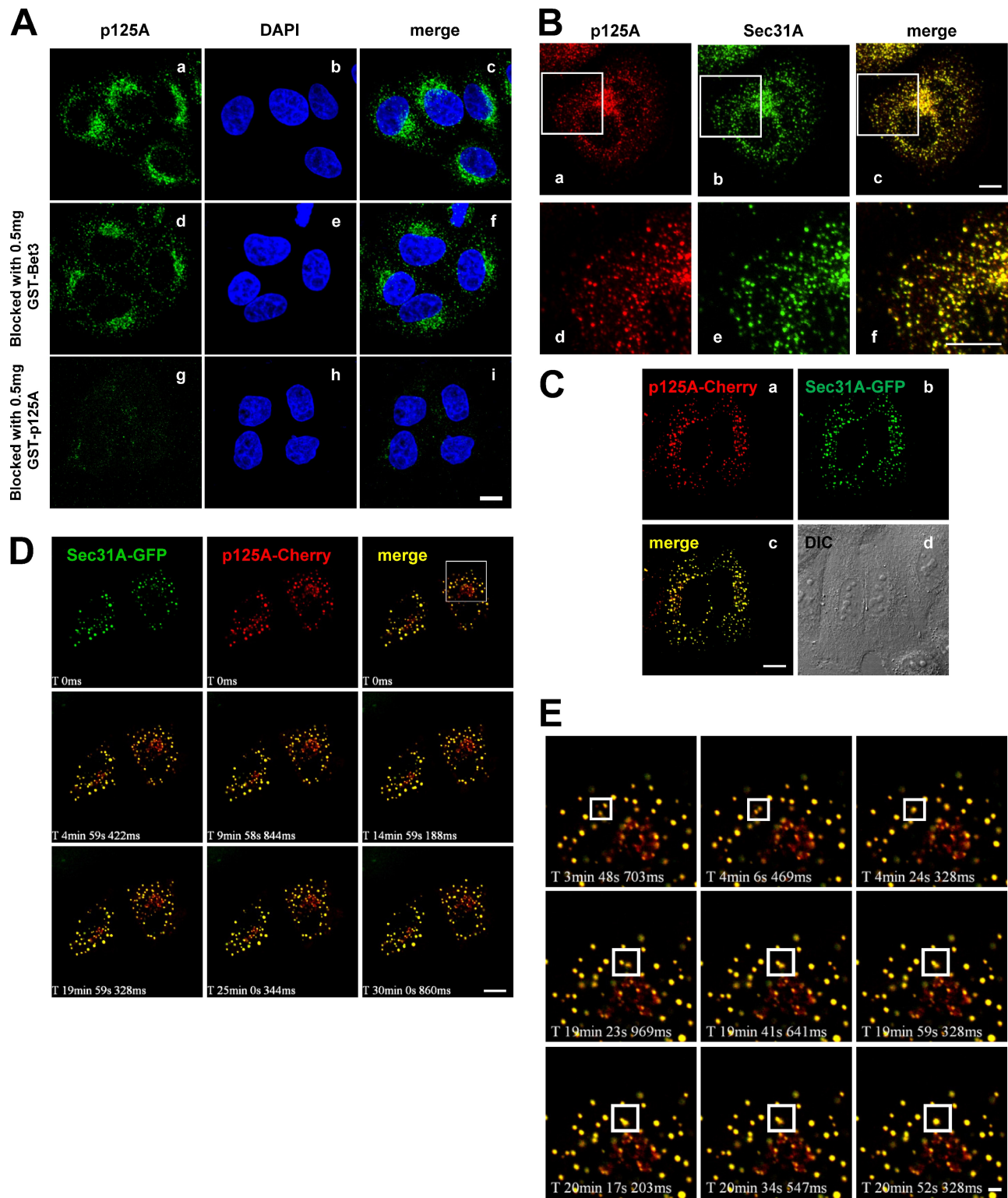


Figure 4. p125A colocalizes extensively with Sec31A. (A) HeLa cells were fixed and labeled with anti-p125A antibodies (a, d, and g) and DAPI (b, e, and h). For the second (d–f) and third (g–i) panels, the antibodies were preincubated with 500 μ g of recombinant GST-Bet3 and GST-p125A, respectively. The merged images are shown in c, f, and i. Bar, 10 μ m. (B) HeLa cells were fixed and double-labeled with rabbit anti-p125A and mouse anti-Sec31A antibodies. Enlarged images of the boxed area are shown in the bottom panels. Bar, 10 μ m. (C) HeLa cells were transfected to coexpress p125A-Cherry (a) and Sec31A-GFP (b). The live cells were imaged with a confocal microscope (Fluoview 1000; Olympus). Merged picture and DIC image are shown in c and d, respectively. Bar, 10 μ m. (D) p125A- and Sec31A-positive structures are colocalized stably with each other over time, and undergo homotypic fusion. HeLa cells were transfected to coexpress p125A-Cherry and Sec31A-GFP. The cells were subjected to live-cell imaging. The vesicular structures of p125A-Cherry colocalize extensively with those of Sec31A-GFP over a period of at least 30 min (Video 1). Inset is enlarged in panels shown in E. Bar, 10 μ m. (E) p125A-Cherry and Sec31A-GFP containing vesicular structures undergo homotypic fusion as indicated by the boxed areas (Video 2). Bar, 2 μ m.

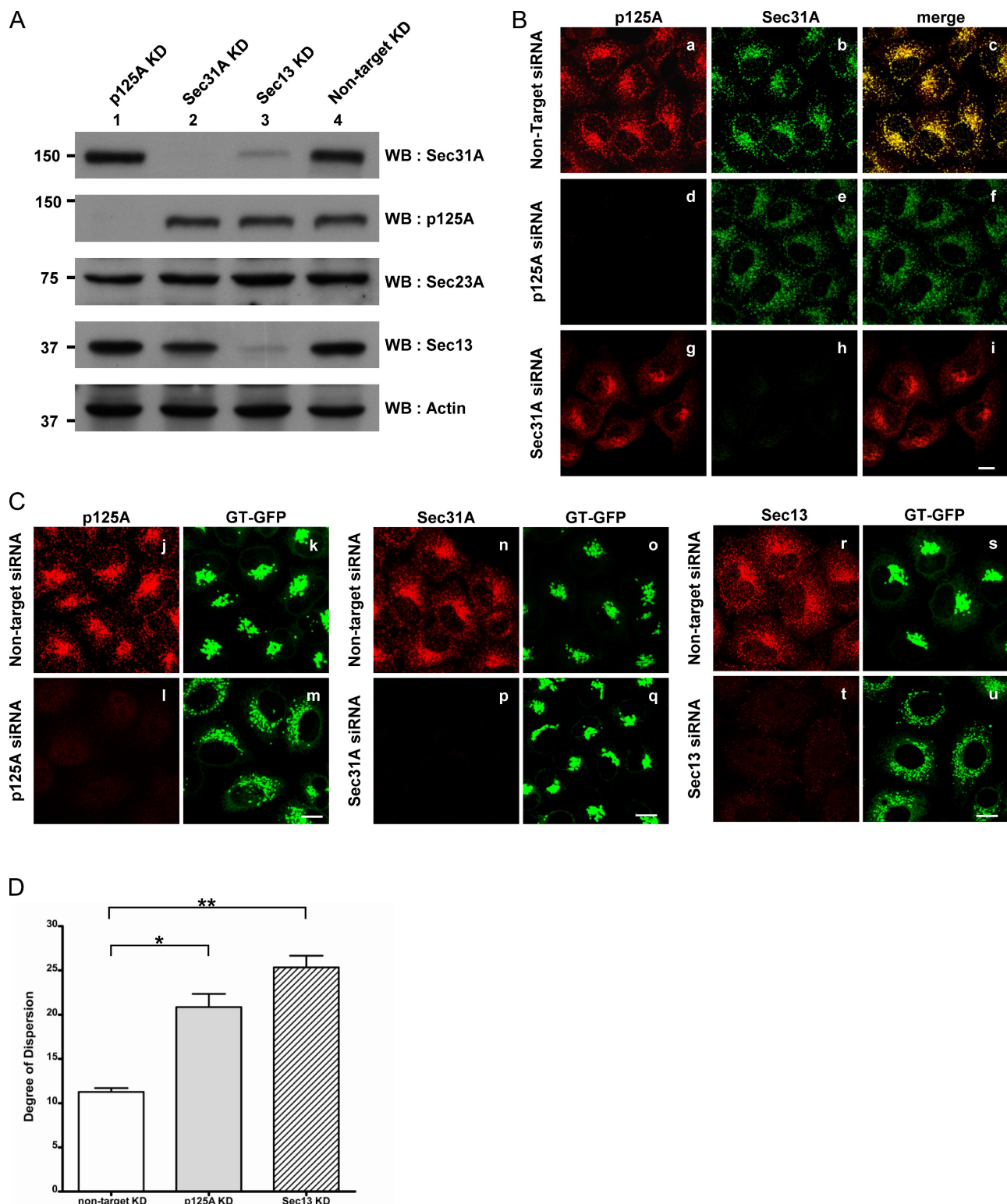


Figure 5. Knockdown of p125A perturbs the structural organization of the early secretory pathway. (A) HeLa cells were transfected twice with ON-Target-plus SMARTpool siRNA (Thermo Fisher Scientific) for p125A, Sec31A, Sec13, or nontarget control with a 24-h interval. 72 h after the initial transfection, cell lysates were prepared and resolved on SDS-PAGE, then subjected to immunoblot analysis using antibodies against Sec31A, p125A, Sec23A, Sec13, and actin. Molecular size markers are in kD. (B) HeLa cells silenced of p125A and Sec31A were double labeled with rabbit anti-p125A and mouse anti-Sec31A antibodies. Bar, 10 μ m. (C) HeLa cells stably expressing GT-GFP were silenced of p125A (left), Sec31A (center), and Sec13 (right). The cells were then processed for indirect immunofluorescence to view GT-GFP as well as p125A, Sec31A, and Sec13, respectively. Bar, 10 μ m. (D) HeLa cells stably expressing GT-GFP were transfected with nontarget, p125A-, or Sec13-specific siRNA. The dispersion and fragmentation of the Golgi marked by GT-GFP were quantified using Cell^P software (Olympus). The open bar represents cells treated with nontarget siRNA, filled bar indicates p125A knockdown cells, and striped bar shows the Sec13 knockdown cells. $n = 15$; *, $P < 0.0001$; **, $P < 0.0001$.

(GT)-GFP (Schaub et al., 2006) (Fig. 5 C). HeLa cells stably expressing GT-GFP were used in this study. In control cells transfected with nontargeting siRNA, GT-GFP was distributed as compact structures characteristic of the Golgi apparatus (panels k, o, and s). In cells silenced of p125A (panel m) or Sec13 (panel u), GT-GFP distribution was aberrant, and appeared as fragmented vesicular structures that scattered more widely around the perinuclear region (panels m and u). Interestingly, in Sec31A-silenced cells (panel q), the general distribution of GT-GFP to the Golgi apparatus was not obviously altered. It was somewhat surprising that knockdown of Sec31A did not achieve a similar phenotype as Sec13 knockdown. One possibility is due to the presence of Sec31B, which shares 47.3% identity to Sec31A and may be able to functionally compensate for the loss of Sec31A (Shugrue et al., 1999; Tang et al., 2000; Stankewich et al., 2006). The extent of Golgi dispersion in response to p125A and Sec13 knockdown was measured and seen to be significantly higher as compared with control cells (Fig. 5 D), suggesting that, like Sec13, p125A is essential for the maintenance of normal Golgi structure.

We next examined the distribution of markers for various subcompartments of the Golgi apparatus in p125A knockdown cells. HeLa cells stably expressing mannosidase II-GFP (ManII-GFP) were used for simultaneous labeling of three Golgi subcompartments: the trans-Golgi marked by endogenous GT (Schaub et al., 2006), the Golgi stack (or *medial* Golgi) marked by ManII-GFP (Velasco et al., 1993), and the cis-Golgi marked by endogenous GM130 (Marra et al., 2007). GT, ManII-GFP, and GM130 were generally colocalized in the compact Golgi apparatus in control cells (Fig. 6 A, a–d). Like GT-GFP, endogenous GT was dispersed into vesicular structures that spread widely when p125A was knocked down (panel e). Similar to GT-marked trans-Golgi, the *medial*-Golgi marked by ManII-GFP (panel f) and cis-Golgi marked by GM130 (panel g) were also fragmented and dispersed into vesicular structures. Higher resolution images showed that the cis-Golgi and trans-Golgi are not completely colocalized but only partially overlapped (panel i). These results suggest that the knockdown of p125A fragmented the compact Golgi apparatus into many mini-Golgi structures, with each containing markers from all three Golgi subcompartments. In spite of their apparent disconnection, these mini-Golgi fragments may still maintain their cis-to-trans organization. The Golgi fragmentation due to p125A knockdown can be rescued by overexpression of myc-p125A (Fig. 6 B). The result suggests that the phenotype produced by p125A knockdown was specific, and the observed Golgi fragmentation is indeed due to reduced levels of endogenous p125A.

ER export was retarded in p125A-silenced cells

Because COPII coat mediates ER export and p125A interacts with COPII components and is enriched in the ERES, p125A may act together with the COPII coat to facilitate ER export. To determine if p125A is involved in COPII-mediated ER export, the ER export of cells treated with p125A RNAi was examined. To assay for ER export, Golgi reassembly in response to brefeldin A (BFA) treatment and washout was measured in HeLa GT-GFP cells.

Before the addition of BFA, GT-GFP in control cells showed compact structures of the Golgi apparatus (Fig. 6 C, a). In the presence of BFA, GT-GFP was distributed to the ER (panel b). Upon removal and washout of BFA, GT-GFP was exported from the ER and became concentrated in the reassembled Golgi apparatus (panels c–f). 30 min after BFA removal, some GT-GFP was found concentrated in post-ER compartments (panel c) and clear Golgi localization of GT-GFP was seen after 45 min of removal (panel d). After 60 min (panels e and f), GT-GFP has essentially redistributed back to the compact Golgi structures.

ER export and distribution of GT-GFP back into mini-Golgi structures were clearly delayed in p125A-silenced cells (Fig. 6 C, bottom panels). GT-GFP was initially localized to fragmented Golgi structures (panel g). Upon BFA treatment, as in control cells, GT-GFP was distributed to the ER (panel h). Even after 30–45 min, the majority of GT-GFP remained in the ER (panels i and j). Some noticeable amount of GT-GFP was seen in post-ER structures after 60 min (panel k). After an additional 30 min (90 min after BFA washout; panel l), GT-GFP was then redistributed back to the mini-Golgi structures. The extents of ER export observed at 60 min (panel k) in p125A-silenced cells were not as obvious and extensive as those observed at 30 min in control cells (panel c), suggesting a delay of ER export of more than 30 min under these conditions. However, from the point of detectable ER export to Golgi redistribution, GT redistribution occurred at comparable kinetics (taking ~30 min) in both control cells (from 30 to 60 min, panels c to e) and p125A-silenced cells (from 60 to 90 min, panels k–l). These results suggest that the delay of Golgi redistribution in p125A-silenced cells is mainly at the point of ER export. Once exported, the rate of redistribution of GT to the Golgi apparatus in control cells and mini-Golgi in p125A-silenced cells is not significantly different. These results suggest that p125A plays an important role specifically in the ER export.

To corroborate a role of p125A in ER export, we monitored the ER export and subsequent transport along the secretory pathway of VSVG. A temperature-sensitive mutant of the VSVG (VSVG-tsO45) tagged with yellow fluorescent protein (VSVG-tsO45-YFP) was used. At the nonpermissive temperature, VSVG-tsO45-YFP is misfolded and accumulated in the ER. Upon shifting to the permissive temperature, VSVG-tsO45-YFP folds properly, and is then exported to the Golgi, en route to the plasma membrane. These characteristics allow us to monitor the synchronized transport of VSVG-tsO45-YFP along the secretory pathway.

We first looked at the distribution of p125A, Sec31A, and VSVG-tsO45-YFP during ER export. The majority of p125A and Sec31A was colocalized in structures characteristic of the ERES. Interestingly, a significant amount of VSVG-tsO45-YFP was found to be colocalized with some of these p125A- and Sec31A-positive ERES after a short period (5 min) of release from the nonpermissive temperature (Fig. 7 A), suggesting that p125A acts together with COPII in the ERES. We next monitored the kinetics of export and subsequent transport of VSVG-tsO45-YFP when p125A was silenced (Fig. 7 B). In control cells, VSVG-tsO45-YFP was clearly present in dispersed perinuclear structures 5 min after release (panel c), and had reached

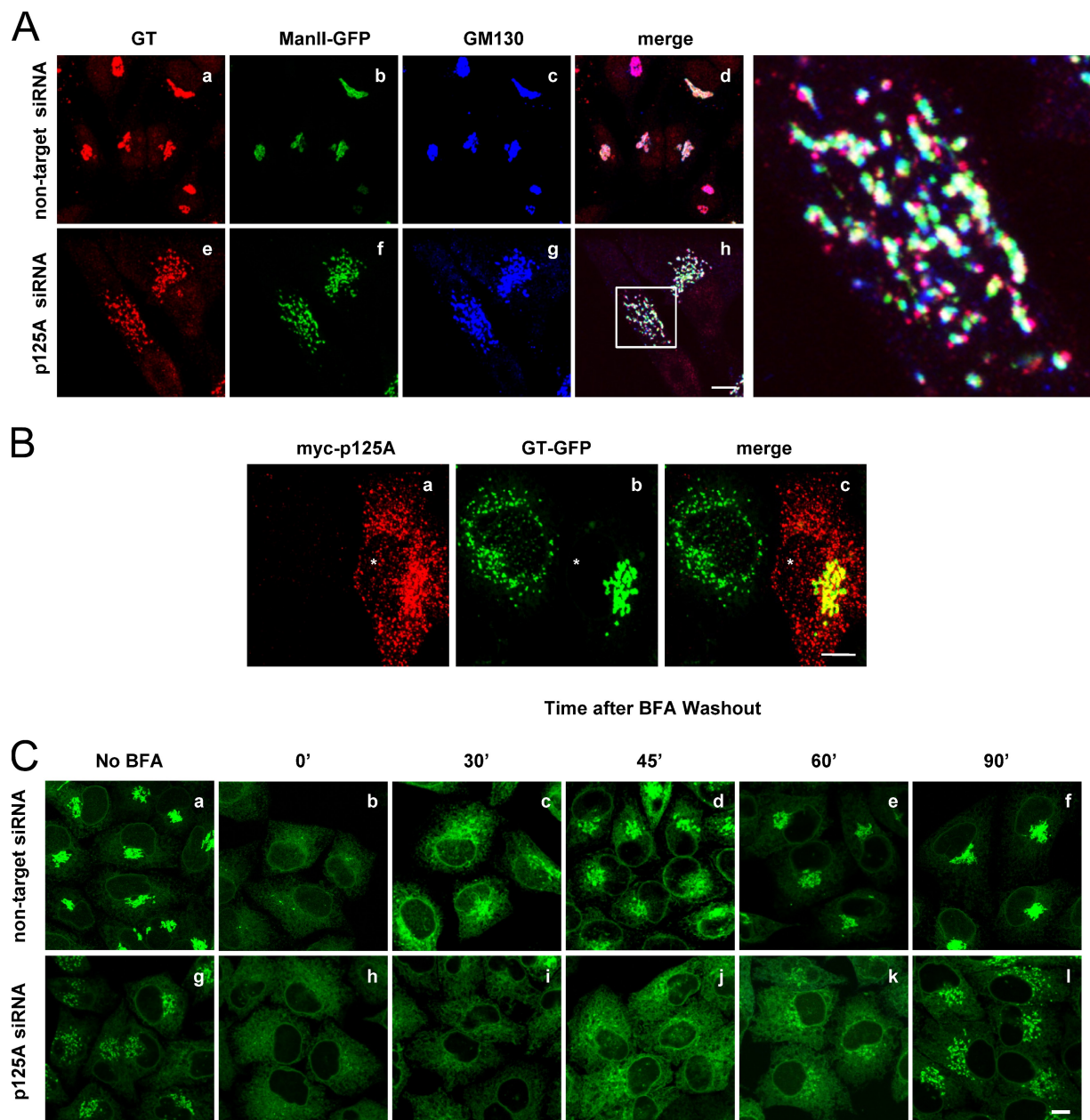


Figure 6. The Golgi apparatus is fragmented into mini-Golgi structures in p125A-silenced cells. (A) HeLa cells stably expressing ManII-GFP were silenced of p125A and then double labeled using mouse anti-GM130 and rabbit anti-GT antibodies followed by viewing the distribution of trans-Golgi marked by GT, medial/Golgi marked by ManII-GFP, and cis-Golgi marked by GM130. Bar, 10 μ m. (B) Exogenous expression of myc-p125A can rescue the dispersed Golgi phenotype in p125A-silenced cells. HeLa cells stably expressing GT-GFP were transfected twice with ON-Targetplus SMARTpool siRNA (Thermo Fisher Scientific) against p125A with a 24-h interval. 48 h after siRNA transfection, the cells were transfected again to express myc-p125A. At 72 h after the initial siRNA transfection, the cells were processed for indirect immunofluorescence microscopy to view GT-GFP and myc-p125A. Asterisk denotes a rescued cell expressing myc-p125A. Bar, 10 μ m. (C) ER export is delayed in p125A-silenced cells. HeLa cells stably expressing GT-GFP were transfected twice either with nontarget or p125A siRNA. At 72 h after the initial transfection, the cells were treated with BFA (5 μ g/ml) for 30 min to distribute GT-GFP into the ER. The cells were then washed and incubated in BFA-free warm medium for the indicated times, and samples were fixed for fluorescence microscopy to assay for ER-Golgi transport of GT-GFP. All of the images were taken at the same exposure and processed in parallel. Bar, 10 μ m.

the Golgi complex by 15–30 min (panels c and d). At 60 min, VSVG-tsO45-YFP was seen to move via vesicular structures from the Golgi for delivery to the surface (panel e). By 120 min, most VSVG-tsO45-YFP had arrived at the plasma membrane (panel f). For p125A-silenced cells, however, VSVG-tsO45-YFP remained essentially in the ER after 5 min release (panel h). At 15 min upon release, VSVG-tsO45-YFP was then seen in perinuclear vesicular structures (panel i) and the majority of

VSVG-tsO45-YFP was present in fragmented mini-Golgi by 30 min. After which, VSVG-tsO45-YFP was seen to be delivered to the plasma membrane (panels k–l). Because the most obvious delay for VSVG-tsO45-YFP transport is at the stage of ER export in p125A-silenced cells, these results further support a role for p125A in COPII-mediated ER export.

We also monitored VSVG-tsO45-YFP transport by a biochemical approach (Fig. 7 C). VSVG-tsO45-YFP is a glycoprotein

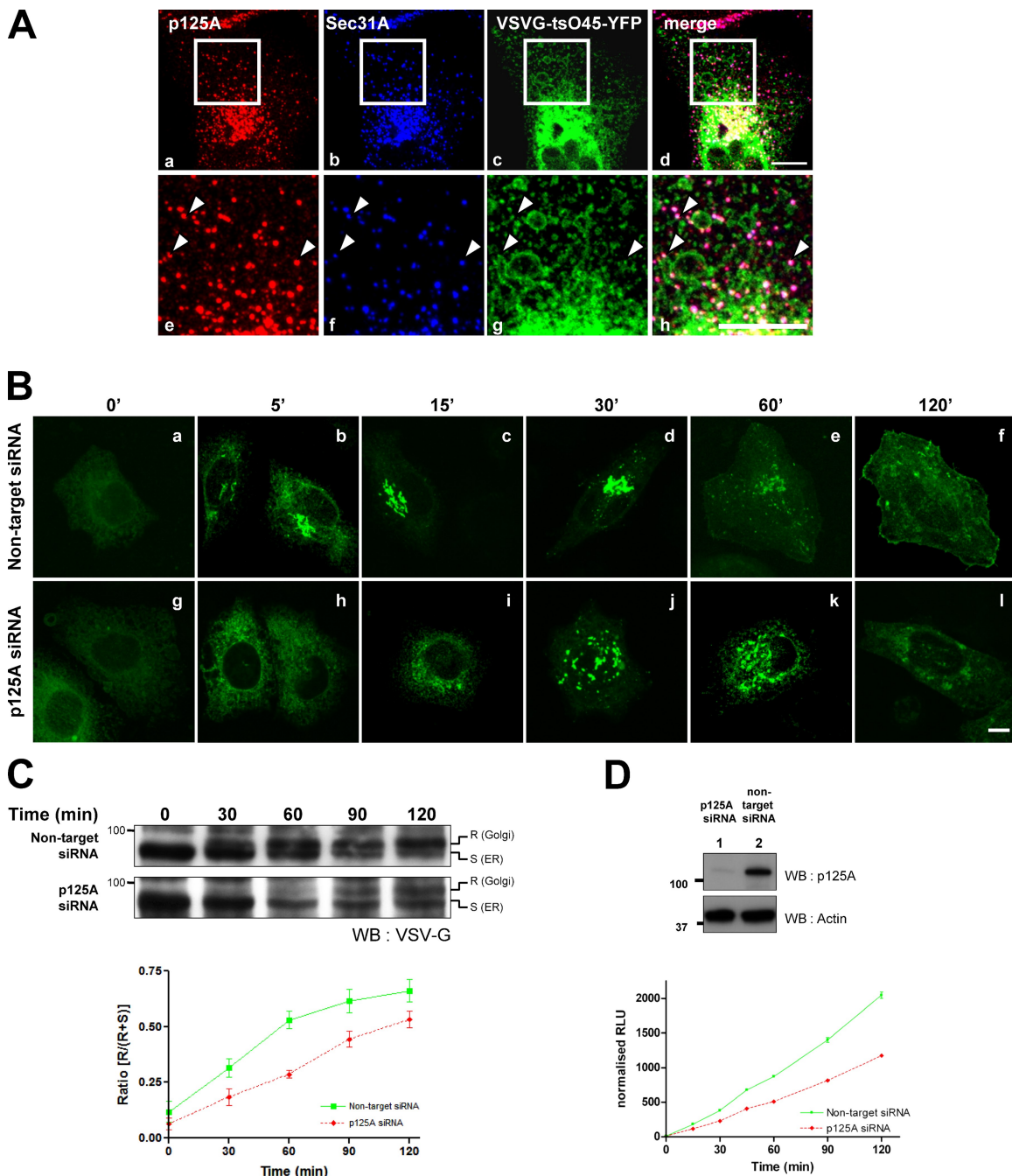


Figure 7. ER-Golgi transport of VSVG-tsO45-YFP is delayed in p125A-silenced cells. (A) HeLa cells were transfected with VSVG-tsO45-YFP and incubated at nonpermissive temperature at 40°C for 24 h. 5 min after release from nonpermissive temperature, the cells were fixed and double labeled with rabbit anti-p125A and mouse anti-Sec31A antibodies. The bottom panels represent the enlarged view of the boxed area in the top panels. The merged images are shown in d and h. Arrowheads indicate colocalization of p125A, Sec31A, and VSVG-tsO45-YFP. Bar, 10 μ m. (B) HeLa cells were transfected twice with ON-Targetplus SMARTpool siRNA (Thermo Fisher Scientific) against p125A or nontarget control. 48 h after the initial transfection, the cells were transfected again to express VSVG-tsO45-YFP at 40°C overnight. At 72 h, the cells were released from 40°C block and incubated at 32°C for various times as indicated. Cells were then processed to view VSVG-tsO45-YFP. Bar, 10 μ m. (C) VSVG-tsO45-YFP acquisition of Endo H resistance is delayed in p125A knockdown cells. HeLa cells silenced of p125A were transfected with VSVG tsO45-YFP plasmid and incubated at 40°C overnight. To allow VSVG-tsO45-YFP transport, the cells were shifted to 32°C. At the indicated times, cell lysate was prepared and subjected to Endo H treatment followed by SDS-PAGE and immunoblotting. R and S denote Endo H-resistant and Endo H-sensitive forms, respectively. The ratio (percentage) of the amount of Endo H-resistant form to that of the total amount (Endo H-resistant + Endo H-sensitive form) was plotted below. Green solid line represents kinetics of acquisition of VSVG tsO45-YFP in nontarget siRNA-treated cells and red dashed lines indicated that in p125A-silenced cells. (D) Secretion of secreted alkaline phosphatase (SEAP) is retarded in p125A-silenced cells. HEK293 cells stably expressing SEAP were transfected with ON-Targetplus SMARTpool siRNA (Thermo Fisher Scientific) for p125A or nontarget control as described in Materials and methods. 72 h after the initial transfection, the cells were washed five times with fresh media (prewarmed to 37°C) and allowed to secrete for various times. Volumes equivalent to 10% of the media were collected at 0, 15, 30, 45, 60, 90, and 120 min. After 120 min, the cells were washed twice with PBS and lysed with 1X SDS sample buffer. 2% cell lysate were analyzed by SDS-PAGE, and then subjected to immunoblot analysis using antibodies against p125A and actin. The collected media was subjected to Chemiluminescent SEAP Assay as described by manufacturer (Takara Bio Inc.) to quantify the amount of SEAP present. The results were then normalized by actin and plotted against time. The experiment was repeated three times. $P < 0.0001$. Molecular size markers are in kD.

and its N-linked glycans become resistant to cleavage by Endo H upon its delivery to the Golgi apparatus. As shown in Fig. 7 C, for control cells (top panel), a significant amount of VSVG-YFP became Endo H resistant at 30 min upon release, and more than half of it became Endo H resistant at 60 min. At 90 and 120 min, most of VSVG-tsO45-YFP was resistant to Endo H. However, the acquisition of Endo H resistance by VSVG-tsO45-YFP was significantly delayed when p125A was knocked down (bottom panel). In addition, secretion of secreted alkaline phosphatase (SEAP) was also retarded when p125A was knocked down (Fig. 7 D), further supporting a role of p125A in the secretory pathway.

Differential centrifugation was performed to determine if p125A is important for membrane association of Sec13/Sec31 heterotetramer (Fig. 8 A). Cytosolic and membrane fractions were obtained from control and p125A knockdown cells and assessed by immunoblot. Syn6 (Bock et al., 1997) and RhoGDI (Fukumoto et al., 1990) were used as the marker for the membrane and cytosol, respectively. The majority of Sec13 and Sec31A were distributed to the membrane fractions in the non-target siRNA control cells. In p125A-silenced cells (Fig. 8 A), almost 40% of Sec13 and Sec31A was distributed to the cytosol as compared with the 5% in the control cells, indicating the importance of p125A in membrane association of Sec13/Sec31.

Discussion

Although p125A was originally identified as an interacting partner for Sec23A (Tani et al., 1999; Mizoguchi et al., 2000; Nakajima et al., 2002; Shimo et al., 2005), our present study has revealed that the majority of cytosolic p125A is actually in complex with the Sec31A/Sec13 subcomplex. This conclusion is based on several observations. First, the majority of endogenous p125A cofractionated with Sec31A and Sec13 by gel filtration analysis as a protein complex with a size of ~600–700 kD. Second, exhaustive, quantitative immunoprecipitations of HA-p125A using anti-HA antibody can effectively and proportionally co-deplete endogenous Sec31A as well as total p125A (the latter consisting of HA-p125A as well as endogenous p125A). Third, HA-p125 and myc-p125A can be both coimmunoprecipitated, together with Sec31A with either anti-HA or anti-myc antibodies. Coimmunoprecipitation of HA-p125 by anti-myc antibody is dependent on the coexpression of myc-p125A or vice versa, suggesting that p125A could potentially form homodimers or oligomers. Because Sec31A/Sec13 exists as heterotetramer and the complex containing p125A, Sec31A, and Sec13 has a size of ~600–700 kD, we favor a model in which p125A, Sec31A, and Sec13 form a heterohexameric complex with two molecules of each in the cytosol, resulting in an estimated size of ~600 kD. Future work using techniques like cryoelectron microscopy will be needed to gain additional insight into this possibility.

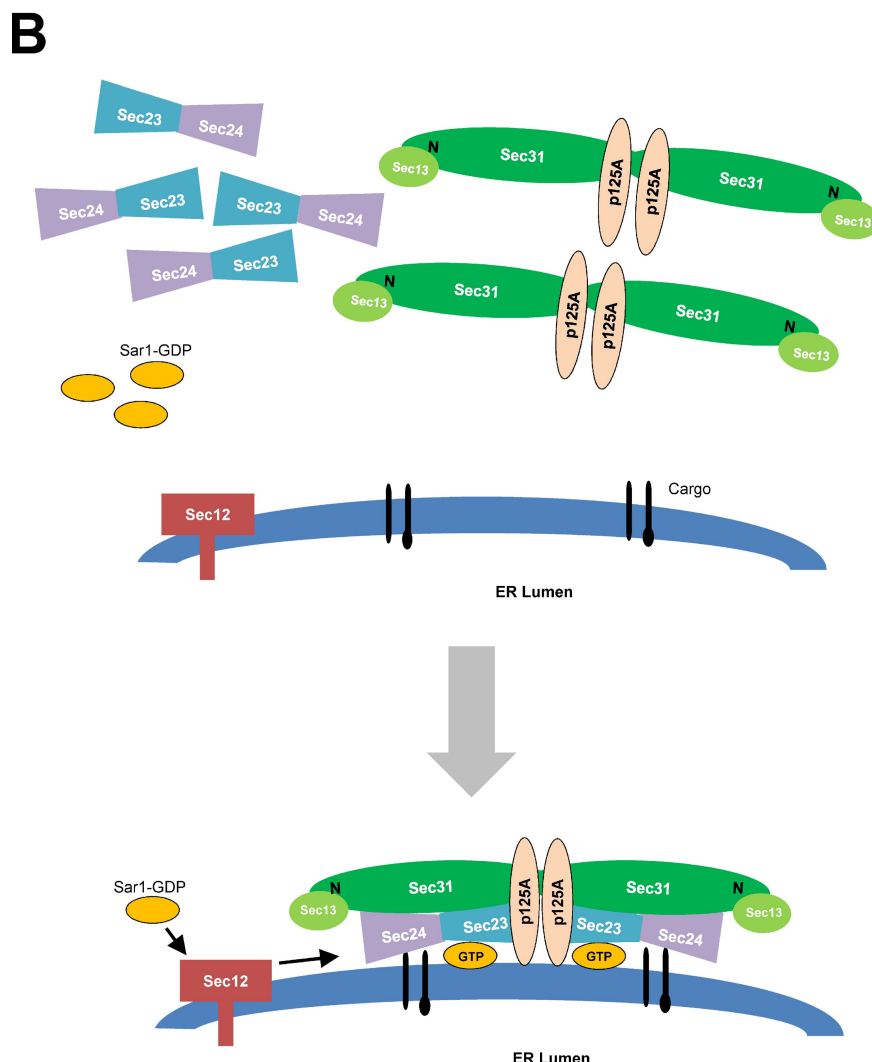
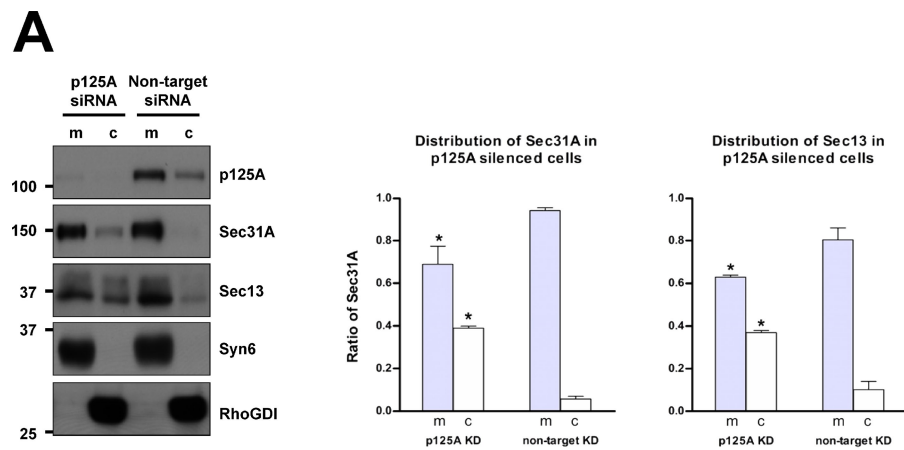
The cellular role of p125A is most consistent with it being an accessory protein for COPII components to facilitate ER export from the ERES. This conclusion is based on several lines of evidence. First, the majority of p125A exists as part of the pre-existing Sec31A/Sec13 subcomplex in the cytosol as mentioned. Second, p125A is enriched in the ERES marked by COPII components such as Sec31A. The colocalization of endogenous

p125A with COPII in the ERES is extensive. Furthermore, exogenous p125A-Cherry and Sec31A-GFP, when coexpressed, displayed almost complete colocalization in structures characteristic of the ERES in both fixed and live cells. Third, export of ER-accumulated GT-GFP as well as VSVG-tsO45-YFP was significantly delayed when endogenous p125A expression was knocked down, whereas post-ER export steps seemed less affected. In support of this notion was the observation that VSVG-tsO45-YFP was colocalized with Sec31A and p125A at structures characteristic of ERES during export. The ability of p125A to interact with Sec31A as well as Sec23A is also most consistent with a role of p125A to act together with COPII coat in ER export.

Although the molecular mechanism underlying p125A action needs further studies, one hypothesis is that it could facilitate the coordination and interaction of the Sec31A/Sec13 subcomplex with the Sec23A/Sec24 subcomplex during the sequential recruitment of different COPII components onto the membrane of ERES (Fig. 8). Because the binding sites for Sec23A and Sec31A are mapped to residues 135–259 and 260–600, respectively, it is possible that p125A can interact simultaneously with both Sec31A and Sec23A at the membrane. Because the majority of p125A exists in complex with Sec31A/Sec13 in the cytosol that is clearly distinct from the complex containing Sec23A, p125A appears not to interact with Sec23A in the cytosol. This is consistent with the observation that immunoprecipitation of p125A did not significantly and proportionally co-deplete Sec23A. However, coimmunoprecipitation of Sec23A with p125A is efficient and robust using total cell lysate (Fig. 2 D). Therefore, it seems likely that during recruitment of p125A/Sec31A/Sec13 heterohexamer onto the membrane-bound Sec23A/Sec24 subcomplex, a conformational change may allow p125A to bind simultaneously with Sec23A and Sec31A to strengthen the interaction between these two COPII subcomplexes to facilitate the formation of COPII vesicles. The molecular structure of the complete COPII cage containing both Sec23/Sec24 and Sec13/Sec31 subcomplexes was recently solved using purified COPII proteins (Stagg et al., 2008). This self-assembled COPII cage appears to have three layers. The innermost layer, which lacks a regular structure, was suggested to contain unassembled Sec13/Sec31 and/or the Sec23/Sec24 subcomplexes. The middle layer comprises the Sec23/Sec24 subcomplex and the outer layer is made up of the Sec13/Sec31 subcomplex. The outer layer did not appear to contact the membrane directly but was membrane bound via interaction(s) with the inner coat (Matsuoka et al., 2001; Lee and Miller, 2007; Stagg et al., 2008). In this context, p125A may potentially strengthen the interaction between the inner and outer layers.

A recent study showed that phosphatidylinositol 4-phosphate can induce the recruitment of the Sec23/Sec24 subcomplex to the membrane by Sar1 in an ATP-independent manner, suggesting that phospholipids have an active role to play in the recruitment of COPII components onto the ERES (Blumental-Perry et al., 2006). p125A contains a phospholipase A1-like domain (Tani et al., 1999) and was found to bind phosphatidylinositol phosphate (Iinuma et al., 2007). It was previously proposed that the phospholipase homology domain of p125A is a primary determinant for

Figure 8. p125A stabilizes the Sec13/Sec31 heterotetramer to the ERES membrane. (A) Membrane (m) and cytosol (c) fractions were obtained from cells transfected with siRNA. Equivalent amounts of each fraction were subjected to SDS-PAGE followed by immunoblot analysis. Molecular size markers are in kD. The intensities of the bands were quantified using Quantity One software (Bio-Rad Laboratories). The ratio of distribution is relative to the total. Total = m (membrane fraction) + c (cytosol fraction). Ratio = m or c/(m+c). The experiment was repeated three times; *, $P < 0.05$. Syntaxin 6 (Syn6) was used as the marker for the membrane fraction and the Rho GDP dissociation inhibitor (RhoGDI) was used as the marker for the cytosolic fraction. (B) A working model to illustrate the role of p125A in ER export in mammalian cells. The majority of p125A, Sec31A, and Sec13 likely exists in the form of a heterohexamer. Upon recruitment of Sar1 and Sec23A/Sec24 subcomplex during COPII vesicle budding, the p125A/Sec31A/Sec13 subcomplex is then recruited, which may open up the binding site of p125A for Sec23A. The simultaneous interaction of p125A with both Sec31A and Sec23A on the budding vesicles may facilitate the coordination of these two COPII subcomplexes to mediate vesicle formation.



membrane attachment (Tani et al., 1999, Shimoi et al., 2005), while the N-terminal region that interacts with Sec23A coordinates membrane specificity (Mizoguchi et al., 2000). In this regard, p125A may also facilitate and strengthen the interaction of COPII components with membrane lipids. Studies along these lines will definitely offer new insights into the detailed mechanism of action of p125A and COPII-mediated export at the ERES in general.

Knockdown of p125A also caused the Golgi apparatus to fragment into many mini-Golgi structures containing markers of cis-, medial-, and trans-subcompartments, which suggest that the cis-trans organization is preserved, whereas stacking or fusion of these structures into compact Golgi ribbons is compromised. Although a direct role for p125A in maintaining the Golgi structure cannot be excluded, we favor the possibility that the observed

Golgi fragmentation and dispersion is an indirect consequence of delayed ER export of some cargo proteins that are important to establish and maintain the compact Golgi structure. Consistent with this notion was the observation that knockdown of Sec13 resulted in a similar and more profound fragmentation and dispersion of the Golgi apparatus. Earlier studies have also shown that depletion of tethering factors and SNAREs that are involved in ER-to-Golgi transport also caused fragmented Golgi structures (Lu et al., 2004; Suga et al., 2005; Marra et al., 2007; Satoh and Warren, 2008; Iinuma et al., 2009). This is also in agreement with the observation that the continual influx of proteins and membrane from the ER to the Golgi is essential for the maintenance of the Golgi ribbon (Shorter and Warren, 1999; Zolov and Lupashin, 2005). Therefore, delayed ER export and reduced anterograde transport from the ER to the Golgi in response to p125A silencing may be the basis for the observed alterations in Golgi morphology. Several studies have shown that even though the integrity of the Golgi was affected in a similar way, secretory cargo could still be delivered to the Golgi complex and beyond, albeit with a lower efficiency (Kondylis and Rabouille, 2003; Marra et al., 2007; Diao et al., 2008). Consistently, we have observed that VGSG transport to the cell surface still occurred when p125A was silenced, although the ER export step was clearly delayed. Collectively, these results suggest that the primary role of p125A is likely one that is within the context of COPII-mediated vesicle budding to facilitate efficient export of cargo proteins from the ER.

Results of our p125A siRNA knockdown seem to differ from what was reported by Shimoi et al. (2005). They did not observe any significant delay in protein export in p125A-silenced cells, whereas we showed that protein export was delayed. To address the discrepancy, we have performed knockdown experiments using their siRNA and transfection condition. Efficient knockdown was seen in only a fraction of cells in which the Golgi apparatus was dispersed, whereas the Golgi apparatus was not significantly affected in surrounding cells that still had detectable levels of p125A (Fig. S1 B, e–h). Using our double-transfection protocol with their siRNA (at higher concentration), more robust knockdown was achieved and the Golgi apparatus was dispersed in most cells (Fig. S1 B, m–p). Similar results were observed when the reassembly of the Golgi apparatus was assessed in response to BFA treatment and washout (Fig. S2). Therefore, the seemingly contradicting results were likely due to the difference in knockdown efficiency of p125A.

Materials and methods

Antibodies

Antibodies were from the following sources: Actin, myc, and HA (Santa Cruz Biotechnology, Inc.); GM130, Rab8, and Sec31A (BD); Syn5 (Synaptic Systems GmbH); Giantin and Sec23A (Abcam); Sec13A (Abnova); β -tubulin and Flag (Sigma-Aldrich); and VSVG (Bethyl Laboratories, Inc.). Fluorochrome-conjugated secondary antibodies were from Invitrogen and HRP-conjugated secondary antibodies were from Jackson ImmunoResearch Laboratories, Inc.

Cell lines

HEK293 and HeLa cells were obtained from American Type Culture Collection (Manassas, VA). HeLa cells stably expressing GT-GFP were a gift from Dr. Jack Rohrer (Friedrich Miescher Institut, Basel, Switzerland). HeLa cells stably expressing ManII-GFP was a gift from Dr. Frederic Bard (Institute of

Molecular Cell Biology, Singapore). 293 cells were grown in DME supplemented with 10% fetal bovine serum (FBS; Hyclone). All HeLa cell lines were cultured in DME-low glucose (1000 mg/L D-glucose) supplemented with 10% FBS and 2 mM L-glutamine (Sigma-Aldrich). HeLa GT-GFP and HeLa ManII-GFP were cultured in the presence of 0.4 mg/ml of G418 (Invitrogen). Cells were cultured at 37°C with 5% CO₂ and 95% humidity.

Other materials

The YFP expressed as fusion with VSVG tsO45 (VSVG-tsO45-YFP) was a gift from Dr. Alexander Mironov (Consorzio Mario Negri Sud, Chieti, Italy). KIAA clones were provided by the Kazusa DNA Research Institute (Chiba, Japan). Expressed sequence tag (EST) clone(s) was obtained from the I.M.A.G.E. consortium via Invitrogen. Brefeldin A (BFA) was purchased from Epicentre Biotechnologies.

Gel filtration

HeLa cytosol was fractionated using the Superose 6 HR 10/30 column (GE Healthcare), using the ÄKTA Purifier 10 FPLC system (GE Healthcare). Fractionation was performed in 25/125 buffer (25 mM Hepes, pH 7.2, and 125 mM potassium acetate) containing 1 mM PMSF at 4°C. Flow rate was 0.3 ml/min and fractions of 0.6 ml each were collected. The fractions were precipitated with trichloroacetic acid (TCA), resolved by SDS-PAGE, and transferred to PVDF membrane (Millipore) for subsequent immunodetection.

Transfection and gene silencing

All plasmid transfections were performed using Effectene (QIAGEN). All siRNA duplexes were of the ON-TARGETplus SMARTpool type obtained from Thermo Fisher Scientific. siRNA duplexes were transfected into HeLa cells using Oligofectamine transfection reagent (Invitrogen) according to the manufacturer's protocol. For efficient expression knockdown, the cells were transfected twice with a 24-h interval. All experiments were performed 72 h after the first siRNA transfection.

Preparation of cytosol and membrane fractions

Cells were harvested and homogenized in cytosol buffer (20 mM Tris-HCl, pH 7.5, 150 mM NaCl, and 1 mM PMSF with complete EDTA-free protease inhibitor mixture [from Roche]). The cell suspension was passed through a 29G needle 10 times on ice. The cell lysate was briefly centrifuged at 2,000 rpm for 5 min at 4°C. The clarified lysate was then subjected to centrifugation at 85,000 rpm using the TLA120.1 rotor (Beckman Coulter) for 1 h at 4°C. Cytosol was collected and the membrane pellet was washed once with cytosol buffer and then centrifuged at 85,000 rpm for 30 min at 4°C once more using the TLA120.1 rotor. The membrane pellet was resuspended in lysis buffer and centrifuged again at 85,000 rpm using the TLA120.1 rotor for 1 h at 4°C for the third time. The solubilized membrane proteins were then collected. The proteins were resolved by SDS-PAGE and transferred to PVDF membrane (Millipore) for subsequent immunodetection.

Immunoprecipitation

Cells on tissue culture dishes were lysed in lysis buffer (20 mM Tris-HCl, pH 7.5, 150 mM NaCl, 1% Triton X-100, and 1 mM PMSF with complete EDTA-free protease inhibitor mixture [Roche]). The lysate was incubated on ice for 30 min and cleared by centrifugation at 13,000 rpm for 30 min at 4°C. Immunoprecipitation was performed at 4°C with 5 μ g of antibody in the presence of either protein A- or protein G-Sepharose 4 Fast Flow (GE Healthcare) for 4 h at 4°C with rotation. The Sepharose was then washed five times with cell lysis buffer and twice with cold PBS. Bound proteins were eluted with 2x Laemmli sample buffer, resolved by SDS-PAGE, and transferred to PVDF membrane (Millipore) for subsequent immunodetection.

Fluorescence microscopy

Cells grown on coverslips (Thermo Fisher Scientific) were washed two times with PBS supplemented with 1 mM CaCl₂ and 1 mM MgCl₂ (PBSCM). The cells were then fixed with 4% paraformaldehyde in PBSCM for 20 min at room temperature. The fixed cells were washed five times at 5-min intervals using PBSCM and then permeabilized with 0.1% Saponin (Sigma-Aldrich) in PBSCM for 20 min at room temperature. The cells were then immunolabeled with appropriate primary antibodies diluted in fluorescence dilution buffer (FDB; PBSCM with 5% FBS and 2% bovine serum albumin [BSA]) for 1 h at room temperature. The coverslips were then washed five times with 0.1% Saponin PBSCM at 5-min intervals. Secondary antibodies were diluted appropriately in FDB and incubated at room temperature for 1 h. The coverslips were washed again with 0.1% Saponin PBSCM five times at

5-min intervals and then twice with PBSCM. The coverslips were mounted on microscopic slides with Vectashield mounting medium containing DAPI (Vector Laboratories). Confocal microscopy was performed with either an Axioplan II microscope (Carl Zeiss, Inc.) equipped with Zeiss confocal scanning optics or a Fluoview 1000 confocal microscope (Olympus).

Live-cell confocal microscopy

Cells were cultured on glass-bottom culture dishes (MatTek) and were transfected with plasmid constructs of interest. The cells were then imaged using the Fluoview 1000 confocal microscope (Olympus).

Golgi reassembly assay

HeLa GT-GFP cells (either grown on coverslips or glass-bottom tissue culture dishes) were treated with a 5- μ g/ml final concentration of BFA (Epicentre Biotechnologies) for 30 min at 37°C. The cells were rinsed five times with warm growth media (37°C) to remove any traces of BFA. The cells were then incubated in growth media at 37°C in the presence of 100 μ g/ml cyclohexamide to inhibit synthesis of new proteins (including GT-GFP fusion). The cells were then fixed and processed for indirect immunofluorescence microscopy after various time points.

VSVG transport assay

siRNA-treated HeLa cells were transfected with VSVG-tsO45-YFP plasmid 48 h after the initial siRNA transfection. Immediately after transfection, the cells were incubated at 40°C to accumulate this temperature-sensitive form of VSVG-tsO45-YFP fusion protein in the ER. After 24 h of incubation at 40°C, the cells were transferred to the permissive temperature at 32°C, upon which the cells were incubated with a final concentration of 100 μ g/ml cyclohexamide to inhibit synthesis of new proteins including VSVG-tsO45-YFP. For the morphological transport assay, the cells were incubated further at 32°C for various times before being fixed with paraformaldehyde and processed for indirect immunofluorescence microscopy. For biochemical transport assay, the cells were incubated further at 32°C for various times before being harvested. Cell lysate was harvested with lysis buffer (0.5% SDS, 1% β -mercaptoethanol) and heated at 100°C for 10 min. Lysate was adjusted to 1x EndoH buffer (50 mM citric acid, pH 5.5). Half of the lysate was treated with 2.5 units of EndoH (Sigma-Aldrich) overnight at 37°C before being analyzed by SDS-PAGE and immunoblot.

Quantification of Golgi dispersion

Confocal images of knockdown and control cells were subjected to analysis using Cell^P software (Olympus). The degrees of Golgi dispersion were calculated based on the distance of the individual vesicular structures/aggregates marked by GT-GFP relative to the center of the dispersed Golgi apparatus. Each aggregate has a coordinate on the confocal image (e.g., X_i, Y_i). The relative center of the Golgi (\bar{X}, \bar{Y}) is the average position of all the aggregates in the selected region of interest. The distance to the relative center of the Golgi was calculated based on the following algorithm:

$$\text{Distance} = \frac{\sum \sqrt{(X_{(1,2,3\dots N)} - \bar{X})^2 + (Y_{(1,2,3\dots N)} - \bar{Y})^2}}{N}$$

Therefore, the further the distance from the relative center of the Golgi, the greater the degree of Golgi dispersion.

Online supplemental material

Fig. S1 shows that different siRNA transfection protocols affect the efficiency of p125A knockdown in HeLa cells. Fig. S2 shows that Golgi reassembles after BFA treatment and washout was delayed in p125A-silenced cells. Video 1 shows that p125A-Cherry and Sec31A-GFP colocalize stably in vesicular structures that appear to undergo homotypic fusion. Video 2 shows a magnified view of Video 1 up to 30 min. Online supplemental material is available at <http://www.jcb.org/cgi/content/full/jcb.201003005/DC1>.

We thank Dr. Alexander Mironov for providing the VSVG-tsO45-YFP construct, Dr. Jack Rohrer for HeLa GT-GFP cells, and Dr. Frederic Bard for HeLa Manl-GFP cells. The KIAA clones were provided by the Kazusa DNA Research Institute. We thank Mr. Raphael Ong for his help in the cloning of fluorescent protein-fused p125A and Sec31A.

Submitted: 1 March 2010

Accepted: 14 July 2010

References

Aridor, M., S.I. Bannykh, T. Rowe, and W.E. Balch. 1995. Sequential coupling between COPII and COPI vesicle coats in endoplasmic reticulum to Golgi transport. *J. Cell Biol.* 131:875–893. doi:10.1083/jcb.131.4.875

Barlowe, C. 2003. Signals for COPII-dependent export from the ER: what's the ticket out? *Trends Cell Biol.* 13:295–300. doi:10.1016/S0962-8924(03)00082-5

Barlowe, C., C. d'Enfert, and R. Schekman. 1993. Purification and characterization of SAR1p, a small GTP-binding protein required for transport vesicle formation from the endoplasmic reticulum. *J. Biol. Chem.* 268:873–879.

Barlowe, C., L. Orci, T. Yeung, M. Hosobuchi, S. Hamamoto, N. Salama, M.F. Rexach, M. Ravazzola, M. Amherdt, and R. Schekman. 1994. COPII: a membrane coat formed by Sec proteins that drive vesicle budding from the endoplasmic reticulum. *Cell.* 77:895–907. doi:10.1016/0092-8674(94)90138-4

Bi, X., J.D. Mancias, and J. Goldberg. 2007. Insights into COPII coat nucleation from the structure of Sec23.Sar1 complexed with the active fragment of Sec31. *Dev. Cell.* 13:635–645. doi:10.1016/j.devcel.2007.10.006

Blumenthal-Perry, A., C.J. Haney, K.M. Weixel, S.C. Watkins, O.A. Weisz, and M. Aridor. 2006. Phosphatidylinositol 4-phosphate formation at ER exit sites regulates ER export. *Dev. Cell.* 11:671–682. doi:10.1016/j.devcel.2006.09.001

Bock, J.B., J. Klumperman, S. Davanger, and R.H. Scheller. 1997. Syntaxin 6 functions in trans-Golgi network vesicle trafficking. *Mol. Biol. Cell.* 8:1261–1271.

Diao, A., L. Frost, Y. Morohashi, and M. Lowe. 2008. Coordination of golgin tethering and SNARE assembly: GM130 binds syntaxin 5 in a p115-regulated manner. *J. Biol. Chem.* 283:6957–6967. doi:10.1074/jbc.M708401200

Ellgaard, L., and A. Helenius. 2003. Quality control in the endoplasmic reticulum. *Nat. Rev. Mol. Cell Biol.* 4:181–191. doi:10.1038/nrm1052

Espenshade, P., R.E. Gimeno, E. Holzmacher, P. Teung, and C.A. Kaiser. 1995. Yeast SEC16 gene encodes a multidomain vesicle coat protein that interacts with Sec23p. *J. Cell Biol.* 131:311–324. doi:10.1083/jcb.131.2.311

Fath, S., J.D. Mancias, X. Bi, and J. Goldberg. 2007. Structure and organization of coat proteins in the COPII cage. *Cell.* 129:1325–1336. doi:10.1016/j.cell.2007.05.036

Fromme, J.C., L. Orci, and R. Schekman. 2008. Coordination of COPII vesicle trafficking by Sec23. *Trends Cell Biol.* 18:330–336. doi:10.1016/j.tcb.2008.04.006

Fukumoto, Y., K. Kaibuchi, Y. Hori, H. Fujioka, S. Araki, T. Ueda, A. Kikuchi, and Y. Takai. 1990. Molecular cloning and characterization of a novel type of regulatory protein (GDI) for the rho proteins, ras p21-like small GTP-binding proteins. *Oncogene.* 5:1321–1328.

Gimeno, R.E., P. Espenshade, and C.A. Kaiser. 1995. SEC4D encodes a yeast endoplasmic reticulum protein that binds Sec16p and participates in vesicle formation. *J. Cell Biol.* 131:325–338. doi:10.1083/jcb.131.2.325

Gimeno, R.E., P. Espenshade, and C.A. Kaiser. 1996. COPII coat subunit interactions: Sec24p and Sec23p bind to adjacent regions of Sec16p. *Mol. Biol. Cell.* 7:1815–1823.

Gorelick, F.S., and C. Shugrue. 2001. Exiting the endoplasmic reticulum. *Mol. Cell Endocrinol.* 177:13–18. doi:10.1016/S0303-7207(01)00438-5

Gürkan, C., S.M. Stagg, P. Lapointe, and W.E. Balch. 2006. The COPII cage: unifying principles of vesicle coat assembly. *Nat. Rev. Mol. Cell Biol.* 7:727–738. doi:10.1038/nrm2025

Hicke, L., T. Yoshihisa, and R. Schekman. 1992. Sec23p and a novel 105-kDa protein function as a multimeric complex to promote vesicle budding and protein transport from the endoplasmic reticulum. *Mol. Biol. Cell.* 3:667–676.

Huber, L.A., S. Pimplikar, R.G. Parton, H. Virta, M. Zerial, and K. Simons. 1993. Rab8, a small GTPase involved in vesicular traffic between the TGN and the basolateral plasma membrane. *J. Cell Biol.* 123:35–45. doi:10.1083/jcb.123.1.35

Hughes, H., and D.J. Stephens. 2008. Assembly, organization, and function of the COPII coat. *Histochem. Cell Biol.* 129:129–151. doi:10.1007/s00418-007-0363-x

Iinuma, T., A. Shiga, K. Nakamoto, M.B. O'Brien, M. Aridor, N. Arimitsu, M. Tagaya, and K. Tani. 2007. Mammalian Sec16/p250 plays a role in membrane traffic from the endoplasmic reticulum. *J. Biol. Chem.* 282:17632–17639. doi:10.1074/jbc.M611237200

Iinuma, T., T. Aoki, K. Arasaki, H. Hirose, A. Yamamoto, R. Samata, H.P. Hauri, N. Arimitsu, M. Tagaya, and K. Tani. 2009. Role of syntaxin 18 in the organization of endoplasmic reticulum subdomains. *J. Cell Sci.* 122:1680–1690. doi:10.1242/jcs.036103

Kim, H.W., P. Yang, Y. Qyang, H. Lai, H. Du, J.S. Henkel, K. Kumar, S. Bao, M. Liu, and S. Marcus. 2001. Genetic and molecular characterization of

Skb15, a highly conserved inhibitor of the fission yeast PAK, Shk1. *Mol. Cell.* 7:1095–1101. doi:10.1016/S1097-2765(01)00248-9

Kirk, S.J., and T.H. Ward. 2007. COPII under the microscope. *Semin. Cell Dev. Biol.* 18:435–447. doi:10.1016/j.semcd.2007.07.007

Kondylis, V., and C. Rabouille. 2003. A novel role for dp115 in the organization of tER sites in *Drosophila*. *J. Cell Biol.* 162:185–198. doi:10.1083/jcb.200301136

Kuehn, M.J., J.M. Herrmann, and R. Schekman. 1998. COPII-cargo interactions direct protein sorting into ER-derived transport vesicles. *Nature.* 391:187–190. doi:10.1038/34438

Kuge, O., C. Dascher, L. Orci, T. Rowe, M. Amherdt, H. Plutner, M. Ravazzola, G. Tanigawa, J.E. Rothman, and W.E. Balch. 1994. Sar1 promotes vesicle budding from the endoplasmic reticulum but not Golgi compartments. *J. Cell Biol.* 125:51–65. doi:10.1083/jcb.125.1.51

Lederkremer, G.Z., Y. Cheng, B.M. Petre, E. Vogan, S. Springer, R. Schekman, T. Walz, and T. Kirchhausen. 2001. Structure of the Sec23p/24p and Sec13p/31p complexes of COPII. *Proc. Natl. Acad. Sci. USA.* 98:10704–10709. doi:10.1073/pnas.191359398

Lee, M.C., and E.A. Miller. 2007. Molecular mechanisms of COPII vesicle formation. *Semin. Cell Dev. Biol.* 18:424–434. doi:10.1016/j.semcd.2007.06.007

Lee, M.C., E.A. Miller, J. Goldberg, L. Orci, and R. Schekman. 2004. Bi-directional protein transport between the ER and Golgi. *Annu. Rev. Cell Dev. Biol.* 20:87–123. doi:10.1146/annurev.cellbio.20.010403.105307

Lu, L., G. Tai, and W. Hong. 2004. Autoantigen Golgin-97, an effector of Arl1 GTPase, participates in traffic from the endosome to the trans-golgi network. *Mol. Biol. Cell.* 15:4426–4443. doi:10.1091/mbc.E03-12-0872

Mancias, J.D., and J. Goldberg. 2005. Exiting the endoplasmic reticulum. *Traffic.* 6:278–285. doi:10.1111/j.1600-0854.2005.00279.x

Marra, P., L. Salvatore, A. Mironov Jr., A. Di Campli, G. Di Tullio, A. Trucco, G. Beznoussenko, A. Mironov, and M.A. De Matteis. 2007. The biogenesis of the Golgi ribbon: the roles of membrane input from the ER and of GM130. *Mol. Biol. Cell.* 18:1595–1608. doi:10.1091/mbc.E06-10-0886

Matsuoka, K., L. Orci, M. Amherdt, S.Y. Bednarek, S. Hamamoto, R. Schekman, and T. Yeung. 1998. COPII-coated vesicle formation reconstituted with purified coat proteins and chemically defined liposomes. *Cell.* 93:263–275. doi:10.1016/S0092-8674(00)81577-9

Matsuoka, K., R. Schekman, L. Orci, and J.E. Heuser. 2001. Surface structure of the COPII-coated vesicle. *Proc. Natl. Acad. Sci. USA.* 98:13705–13709. doi:10.1073/pnas.241522198

Mizoguchi, T., K. Nakajima, K. Hatsuzawa, M. Nagahama, H.P. Hauri, M. Tagaya, and K. Tani. 2000. Determination of functional regions of p125, a novel mammalian Sec23p-interacting protein. *Biochem. Biophys. Res. Commun.* 279:144–149. doi:10.1006/bbrc.2000.3846

Nakajima, K., H. Sonoda, T. Mizoguchi, J. Aoki, H. Arai, M. Nagahama, M. Tagaya, and K. Tani. 2002. A novel phospholipase A1 with sequence homology to a mammalian Sec23p-interacting protein, p125. *J. Biol. Chem.* 277:11329–11335. doi:10.1074/jbc.M111092200

Nakano, A., and M. Muramatsu. 1989. A novel GTP-binding protein, Sar1p, is involved in transport from the endoplasmic reticulum to the Golgi apparatus. *J. Cell Biol.* 109:2677–2691. doi:10.1083/jcb.109.6.2677

Saito-Nakano, Y., and A. Nakano. 2000. Sed4p functions as a positive regulator of Sar1p probably through inhibition of the GTPase activation by Sec23p. *Genes Cells.* 5:1039–1048. doi:10.1046/j.1365-2443.2000.00391.x

Salama, N.R., T. Yeung, and R.W. Schekman. 1993. The Sec13p complex and reconstitution of vesicle budding from the ER with purified cytosolic proteins. *EMBO J.* 12:4073–4082.

Salama, N.R., J.S. Chuang, and R.W. Schekman. 1997. Sec31 encodes an essential component of the COPII coat required for transport vesicle budding from the endoplasmic reticulum. *Mol. Biol. Cell.* 8:205–217.

Satoh, A., and G. Warren. 2008. In situ cleavage of the acidic domain from the p115 tether inhibits exocytic transport. *Traffic.* 9:1522–1529. doi:10.1111/j.1600-0854.2008.00783.x

Schaub, B.E., B. Berger, E.G. Berger, and J. Rohrer. 2006. Transition of galactosyltransferase 1 from trans-Golgi cisterna to the trans-Golgi network is signal mediated. *Mol. Biol. Cell.* 17:5153–5162. doi:10.1091/mbc.E06-08-0665

Shaywitz, D.A., P.J. Espenshade, R.E. Gimeno, and C.A. Kaiser. 1997. COPII subunit interactions in the assembly of the vesicle coat. *J. Biol. Chem.* 272:25413–25416. doi:10.1074/jbc.272.41.25413

Shimoji, W., I. Ezawa, K. Nakamoto, S. Uesaki, G. Gabreski, M. Aridor, A. Yamamoto, M. Nagahama, M. Tagaya, and K. Tani. 2005. p125 is localized in endoplasmic reticulum exit sites and involved in their organization. *J. Biol. Chem.* 280:10141–10148. doi:10.1074/jbc.M409673200

Shorter, J., and G. Warren. 1999. A role for the vesicle tethering protein, p115, in the post-mitotic stacking of reassembling Golgi cisternae in a cell-free system. *J. Cell Biol.* 146:57–70.

Shugrue, C.A., E.R. Kolen, H. Peters, A. Czernik, C. Kaiser, L. Matovcik, A.L. Hubbard, and F. Gorelick. 1999. Identification of the putative mammalian orthologue of Sec31P, a component of the COPII coat. *J. Cell Sci.* 112:4547–4556.

Siegel, L.M., and K.J. Monty. 1966. Determination of molecular weights and frictional ratios of proteins in impure systems by use of gel filtration and density gradient centrifugation. Application to crude preparations of sulfite and hydroxylamine reductases. *Biochim. Biophys. Acta.* 112:346–362. doi:10.1016/0926-6585(66)90333-5

Stagg, S.M., C. Gürkan, D.M. Fowler, P. LaPointe, T.R. Foss, C.S. Potter, B. Carragher, and W.E. Balch. 2006. Structure of the Sec13/31 COPII coat cage. *Nature.* 439:234–238. doi:10.1038/nature04339

Stagg, S.M., P. LaPointe, A. Razvi, C. Gürkan, C.S. Potter, B. Carragher, and W.E. Balch. 2008. Structural basis for cargo regulation of COPII coat assembly. *Cell.* 134:474–484. doi:10.1016/j.cell.2008.06.024

Stankewich, M.C., P.R. Stabach, and J.S. Morrow. 2006. Human Sec31B: a family of new mammalian orthologues of yeast Sec31p that associate with the COPII coat. *J. Cell Sci.* 119:958–969. doi:10.1242/jcs.02751

Suga, K., H. Hattori, A. Saito, and K. Akagawa. 2005. RNA interference-mediated silencing of the syntaxin 5 gene induces Golgi fragmentation but capable of transporting vesicles. *FEBS Lett.* 579:4226–4234. doi:10.1016/j.febslet.2005.06.053

Supek, F., D.T. Madden, S. Hamamoto, L. Orci, and R. Schekman. 2002. Sec16p potentiates the action of COPII proteins to bud transport vesicles. *J. Cell Biol.* 158:1029–1038. doi:10.1083/jcb.200207053

Tang, B.L., T. Zhang, D.Y. Low, E.T. Wong, H. Horstmann, and W. Hong. 2000. Mammalian homologues of yeast sec31p. An ubiquitously expressed form is localized to endoplasmic reticulum (ER) exit sites and is essential for ER-Golgi transport. *J. Biol. Chem.* 275:13597–13604. doi:10.1074/jbc.275.18.13597

Tani, K., T. Mizoguchi, A. Iwamatsu, K. Hatsuzawa, and M. Tagaya. 1999. p125 is a novel mammalian Sec23p-interacting protein with structural similarity to phospholipid-modifying proteins. *J. Biol. Chem.* 274:20505–20512. doi:10.1074/jbc.274.29.20505

Velasco, A., L. Hendricks, K.W. Moremen, D.R. Tulsiani, O. Touster, and M.G. Farquhar. 1993. Cell type-dependent variations in the subcellular distribution of alpha-mannosidase I and II. *J. Cell Biol.* 122:39–51. doi:10.1083/jcb.122.1.39

Zolov, S.N., and V.V. Lupashin. 2005. Cog3p depletion blocks vesicle-mediated Golgi retrograde trafficking in HeLa cells. *J. Cell Biol.* 168:747–759. doi:10.1083/jcb.200412003